JOURNAL OF GUIDANCE, CONTROL, AND DYNAMICS
Vol. 16, No. 6, November–December 1993

Component Modes Damping Assignment Methodology for Articulated, Multiflexible Body Structures

Allan Y. Lee*
Jet Propulsion Laboratory, California Institute of Technology, Pasadena, California 91109

To simulate the dynamical motion of articulated, multiflexible body structures, one can use multibody simulation packages such as DISCOS. To this end, one must supply appropriate reduced-order models for all of the flexible components involved. The component modes projection and assembly model reduction (COMPARE) methodology is one way to construct these reduced-order component models, which when reassembled capture important system input-to-output mapping of the full-order model at multiple system configurations of interest. In conjunction, we must also supply component damping matrices which when reassembled generate a system damping matrix that has certain desirable properties. The problem of determining the damping factors of components' modes to achieve a given system damping matrix is addressed here. To this end, we must establish from first principles a matrix-algebraic relation between the system's modal damping matrix and the components' modal damping matrices. An unconstrained/constrained optimization problem can then be formulated to determine the component modes' damping factors that best satisfy that matrix-algebraic relation. The effectiveness of the developed methodology, called ModeDamp, has been successfully demonstrated on a high-order, finite element model of the Galileo spacecraft.

I. Background and Motivation

TO simulate and analyze the dynamical motion of articulated, multiflexible body structures, one can use multibody simulation packages such as DISCOS.[1] To this end, one must supply appropriate reduced-order models for all of the flexible components involved, together with the relevant component damping matrices. For complex systems such as the Galileo spacecraft, practical considerations (e.g., simulation time) impose limits on the number of modes that each flexible body can retain in a given simulation. Modal truncation procedures must be used to select and retain a limited number of important modes that capture the salient features of the system dynamics. The enhanced projection and assembly model reduction methodology[2] and the component modes projection and assembly model reduction methodology[3] are two effective ways of generating reduced-order component models for articulated, multiflexible body structures.

The component modes projection and assembly model reduction methodology,[3] to be reviewed in Sec. II, is a two-stage model reduction methodology, combining the classical component mode synthesis method and the newly developed enhanced projection and assembly method. This methodology can generate reduced-order component models that, when reassembled using the interface compatibility conditions, generate a reduced-order system model that exactly captured a number of system modes of interest as well as the static gain of an input/output pair of the full-order system. The effectiveness of this methodology has been successfully verified using a high-order, cruise-configured Galileo spacecraft model.

This component model reduction methodology, like other methodologies, generates reduced-order system models with extraneous modes. How these unwanted modes are generated may be understood as follows. Assume we have a two flexible body structure with the bodies connected via a single-degree-of-freedom (DOF) hinge. We further assume that using a mode selection criterion, 20 important system modes were selected to be retained in the reduced-order system model. Using this methodology, the 20-mode mode set is then augmented with one static correction mode. (The need for the addition of this static correction mode will be explained in Sec. II.) The 21-mode mode set is then projected onto the two component models. When the resultant reduced-order component models are reassembled, the reduced-order system will have 37 ($21+21-5$; a single DOF hinge corresponds to 5 constraints) modes. These 37 modes include the 20 desired system modes together with 17 "extraneous" modes.

Experience indicates that many of these extraneous modes are high frequency in nature, i.e., they lie well outside the frequency range of interest.[2,3] To numerically integrate a reduced-order system model whose highest frequency extraneous modes is ω_e (rad/s), a step size smaller than $\Delta = C/\omega_e$ must be used to avoid numerical instability problems (the constant $C=2.83$ when we use the explicit fourth-order Runge-Kutta algorithm). Therefore, a reduced-order model with one or more high-frequency extraneous mode(s) will significantly increase the elapsed time of integrating the equations of motion of that model.

A two-pronged approach can be used to deal with these unwanted extraneous modes. First, high-frequency extraneous modes should be eliminated whenever possible. Techniques that can be used to eliminate high-frequency extraneous modes (but at the expense of producing a reduced-order system model with degraded fidelity) were suggested in Ref. 4. High-frequency extraneous modes that cannot be eliminated and extraneous modes that fall within the frequency range of interest can still degrade the fidelity of the free or forced time responses of the reduced-order system model. They can be dealt with by assigning larger damping factors to these extraneous modes.

The treatment of damping in complex structures has always posed difficult problems. Owing to the variety of different mechanisms that contribute to damping and to the general lack of knowledge regarding many of them, it has not been possible to model damping on a finite element basis the way mass and stiffness are modeled. For simplicity, it is a common practice to introduce damping only after equations (for each component) have been transformed to modal coordinates. In this case, some reasonable level of viscous damping is typically assumed, and the modal damping matrix is usually taken to be

Received Oct. 25, 1992; revision received Feb. 4, 1993; accepted for publication Feb. 16, 1993.

*Member of Technical Staff, Guidance and Control Section.

diagonal. These component-level damping characteristics are then combined (see, e.g., techniques described in Refs. 5–7; results obtained using these techniques and those found experimentally are compared in Ref. 8) to produce the system damping matrix.

From experience obtained from working with today's space structures, a uniform damping factor of not more than 0.25% can usually be conservatively assumed for all of the system modes.[9,10] (In Ref. 9, a uniform damping factor of 0.50% has been assumed for all of the structural modes.) The system damping matrix obtained by combining reasonable levels of component dampings might or might not adhere to this rule of thumb. If it does not, a time consuming, iterative procedure must then be used to adjust the damping factors of the component modes until it does. Reference 10 describes a technique in which the partial derivative of each system mode's damping with respect to each and every component modes' dampings are evaluated and used to improve the convergence of the iterative process.

This paper addresses the issue of determining the component damping matrices that when reassembled give a system damping matrix with certain desirable properties. When properly implemented, such a technique aids dynamicists in their studies of the damped dynamics of interconnected flexible bodies using multibody simulation packages.

II. Component Modes Projection and Assembly Model Reduction Methodology Revisited

Before we embark on describing the component modes damping assignment technique, let us first review the component modes projection and assembly model reduction (COMPARE) methodology.[3] This is a two-stage model reduction methodology, combining the classical component mode synthesis (CMS) method and the newly developed enhanced projection and assembly method (EP&A). A graphical illustration of the steps involved in the COMPARE model reduction methodology is depicted in Fig. 1.

Step 1 (see Fig. 1) of COMPARE involves the generations of CMS mode sets, such as the MacNeal-Rubin or Craig-Brampton mode sets. Methods commonly used in generating these mode sets are well documented; see, e.g., Ref. 11. These mode sets are then used to reduce the order of each component model in the Rayleigh-Ritz sense. The resultant component models when assembled using the interface compatibility conditions generate system models at various system configurations of interest (cf., step 2 in Fig. 1).

To illustrate step 2, consider a system with two flexible components. The undamped motion of component A in modal coordinates is given by

$$I_{pp}\ddot{\eta}_p^A + \Lambda_{pp}^A\eta_p^A = G_{pa}^A u_a^A, \qquad y_b^A = H_{bp}^A\eta_p^A \tag{1}$$

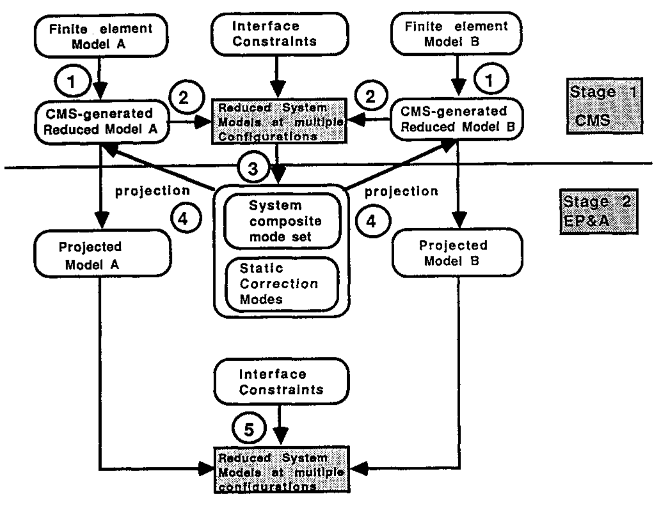

Fig. 1 Graphical illustration of the COMPARE stages.

Here η_p^A and Λ_{pp}^A are the modal coordinates and the diagonal stiffness matrix of component A, respectively. Note that the dimension(s) of the matrix is indicated by its subscript(s). For example, the matrix G_{pa}^A is a $p \times a$ control distribution matrix, and u_a^A is an $a \times 1$ control vector. Similarly, the matrix H_{bp}^A is an output distribution matrix, and y_b^A an output vector. Similar equations for component B are

$$I_{qq}\ddot{\eta}_q^B + \Lambda_{qq}^B\eta_q^B = G_{qa}^B u_a^B, \qquad y_l^B = H_{lq}^B\eta_q^B \tag{2}$$

Here q is the dimension of the CMS mode set of component B.

The system equations of motion at a particular configuration angle α could be constructed using these component equations and enforcing i interface compatibility conditions. To this end, let $P(\alpha) = [P_{pe}^{A^T}(\alpha), P_{qe}^{B^T}(\alpha)]^T$ be a full-rank matrix mapping a minimal system state η_e into

$$\begin{bmatrix} \eta_p^A \\ \eta_q^B \end{bmatrix} = \begin{bmatrix} P_{pe}^A(\alpha) \\ P_{qe}^B(\alpha) \end{bmatrix} [\eta_e] \tag{3}$$

where η_e is an $e \times 1$ system coordinate ($e = p + q - i$). One way to obtain $P_{pe}^A(\alpha)$ and $P_{qe}^B(\alpha)$, using the system interface compatibility relations, will be described in subsequent sections of this paper [cf., Eqs. (11–14)]. For ease of notation, the dependencies of the matrices P_{pe}^A, P_{qe}^B, η_p^A, η_q^B, and η_e on α are dropped in the sequel. From Eqs. (1–3), the system equations of motion are

$$M_{ee}\ddot{\eta}_e + K_{ee}\eta_e = G_{ea}u_a \tag{4}$$

$$y_s = H_{se}\eta_e \tag{5}$$

where $y_s = [y_b^{A^T} \quad y_l^{B^T}]^T$, and $s = b + l$. In Eqs. (4) and (5),

$$M_{ee} = P_{pe}^{A^T}P_{pe}^A + P_{qe}^{B^T}P_{qe}^B$$

$$K_{ee} = P_{pe}^{A^T}\Lambda_{pp}^A P_{pe}^A + P_{qe}^{B^T}\Lambda_{qq}^B P_{qe}^B$$

$$G_{ea} = P_{pe}^{A^T}G_{pa}^A + P_{qe}^{B^T}G_{qa}^B$$

$$H_{se} = [P_{pe}^{A^T}H_{bp}^{A^T} \; P_{qe}^{B^T}H_{lq}^{B^T}]^T$$

To arrive at the expression for G_{ea}, we have assumed that $u_a^A = u_a^B = u_a$. Otherwise, the term $G_{ea}u_a$ in Eq. (4) should be replaced by

$$[P_{pe}^{A^T}\, G_{pa}^A \; P_{qe}^{B^T}\, G_{qa}^B][u_a^{A^T} \; u_a^{B^T}]^T$$

Let $(\Phi_{ee}, \Lambda_{ee}) = \mathrm{eig}(K_{ee}, M_{ee})$ and Eqs. (4) and (5) become

$$\begin{aligned} I_{ee}\ddot{\phi}_e + \Lambda_{ee}\phi_e &= \Phi_{ee}^T G_{ea}u_a \\ y_s &= H_{se}\Phi_{ee}\phi_e \end{aligned} \tag{6}$$

where ϕ_e is the generalized coordinate, i.e., $\eta_e = \Phi_{ee}\phi_e$, $\Phi_{ee}^T M_{ee}\Phi_{ee} = I_{ee}$, and $\Lambda_{ee} = \Phi_{ee}^T K_{ee}\Phi_{ee}$, a diagonal matrix with the undamped, reduced-order system eigenvalues down its diagonal.

The second stage of the COMPARE methodology uses the EP&A method.[2] In applying the EP&A methodology, only k of the system's e modes are kept whereas the remaining t ($= e - k$) modes are removed (see step 3 in Fig. 1). The kept mode set is a composite mode set, consisting of important system modes from all of the system configurations of interest and not just from one particular configuration. This composite mode set approach has been proven to be effective in capturing important modes at all of the system configurations of interest.[12] With this understanding, we have

$$\eta_e = \Phi_{ee}\phi_e \triangleq [\Phi_{ek} \quad \Phi_{et}]\begin{bmatrix} \phi_k \\ \phi_t \end{bmatrix} \doteq \Phi_{ek}\phi_k \tag{7}$$

where ϕ_k and ϕ_t are the kept and truncated coordinates, respectively.

Before the composite mode set Φ_{ek} is projected onto the CMS-based component models (1) and (2), it must first be augmented with static correction modes Φ_{ea}. Although the dimension of the composite mode set is slightly increased by these added modes, they ensure that the static gain of the full-order system from a given input to an output is preserved in the reduced-order system model. One way to generate these static correction modes Φ_{ea} was described in Ref. 12. The projections of the augmented composite mode set $\Phi_{em} \triangleq [\Phi_{ek}\Phi_{ea}]$, $m = k + a$, onto the CMS-based models are accomplished using (cf., step 4)

$$\eta_p^A \doteq P_{pe}^A \Phi_{em} \phi_m^A \triangleq \Psi_{pm}^A \phi_m^A$$
$$\eta_q^B \doteq P_{qe}^B \Phi_{em} \phi_m^B \triangleq \Psi_{qm}^B \phi_m^B \tag{8}$$

where ϕ_m^A and ϕ_m^B denote reduced sets of generalized coordinates of components A and B, respectively. Substitutions of Eq. (8) into Eqs. (1) and (2) produce the "constrained" equations of motion for the respective components

$$\Psi_{pm}^{A^T}\Psi_{pm}^A\ddot{\phi}_m^A + \Psi_{pm}^{A^T}\Lambda_{pp}^A\Psi_{pm}^A\phi_m^A = \Psi_{pm}^{A^T}G_{pa}^A u_a^A$$
$$\Psi_{qm}^{B^T}\Psi_{qm}^B\ddot{\phi}_m^B + \Psi_{qm}^{B^T}\Lambda_{qq}^B\Psi_{qm}^B\phi_m^B = \Psi_{qm}^{B^T}G_{qa}^B u_a^B \tag{9}$$

In general, neither the reduced mass nor stiffness matrices in Eq. (9) is diagonal. To diagonalize these matrices, two eigenvalue problems associated with Eq. (9) are solved. Let Ξ_{mm}^A and Ξ_{mm}^B be the mass-normalized eigenvector matrices obtained, and ν_m^A and ν_m^B be the corresponding generalized coordinates. Substitutions of $\phi_m^A = \Xi_{mm}^A\nu_m^A$ and $\phi_m^B = \Xi_{mm}^B\nu_m^B$ into Eq. (9) give

$$I_{mm}^A\ddot{\nu}_m^A + C_{mm}^A\dot{\nu}_m^A + \Lambda_{mm}^A\nu_m^A = \Pi_{pm}^{A^T}G_{pa}^A u_a^A$$
$$I_{mm}^B\ddot{\nu}_m^B + C_{mm}^B\dot{\nu}_m^B + \Lambda_{mm}^B\nu_m^B = \Pi_{qm}^{B^T}G_{qa}^B u_a^B \tag{10}$$

in Eq. (10), $\Pi_{pm}^A \triangleq \Psi_{pm}^A\Xi_{mm}^A$, and $\Lambda_{mm}^A = \Pi_{pm}^{A^T}\Lambda_{pp}^A\Pi_{pm}^A$ is a diagonal eigenvalue matrix of the reduced-order component A model, with the eigenvalues arranged in ascending order down its diagonal. Similar expressions could also be written for Π_{qm}^B and Λ_{mm}^B.

In Eq. (10), modal damping terms $C_{mm}^A\dot{\nu}_m^A$ and $C_{mm}^B\dot{\nu}_m^B$, usually assumed in the studies of lightly damped structures, have been added. However, it should always be remembered that they are simplified mathematical representations of a rather complex situation that might include other forms of energy dissipation such as coulomb damping, hysteresis damping, etc. The hypothesis is that if the damping in a system is small, these various damping effects can be grossly represented by the diagonally dominant viscous damping matrices C_{mm}^A and C_{mm}^B in Eq. (10). However, it should be pointed out that the "diagonal" assumption has been made only for convenience, and that the component modes damping assignment techniques, to be described in Sec. III, is equally applicable in cases where C_{mm}^A and C_{mm}^B are nondiagonal.

In the last step (step 5), the reduced-order system equations of motion at a particular system configuration α are formed by enforcing displacement compatibility at the interface

$$N_{ip}^A\eta_p^A + N_{iq}^B\eta_q^B = 0 \tag{11}$$

where N_{ip}^A and N_{iq}^B are matrices that establish the constraint relations between the modal coordinates of CMS-generated component models. Using Eqs. (8) and (10), Eq. (11) becomes

$$[N_{ip}^A\Pi_{pm}^A \quad N_{iq}^B\Pi_{qm}^B]\begin{bmatrix}\nu_m^A\\ \nu_m^B\end{bmatrix} \triangleq [D_{ic}]\begin{bmatrix}\nu_m^A\\ \nu_m^B\end{bmatrix} \doteq 0 \tag{12}$$

Here, $[D_{ic}]$ is a compatibility matrix, and $c = 2m$. To construct the reduced-order system model, we partition $[D_{ic}]$ using the singular value decomposition (SVD) technique

$$[D_{ic}] = [U_{ii}][\Sigma_{ii}, O_{id}]\begin{bmatrix}P_{ci}^T\\ P_{cd}^T\end{bmatrix} \tag{13}$$

where $d = c - i$, Σ_{ii} is an $i \times i$ diagonal matrix with i singular values of the matrix D_{ic} along its diagonal, and O_{id} is an $i \times d$ null matrix. The partitioned matrix P_{cd} in Eq. (13) can be used as follows[3,13]:

$$\begin{bmatrix}\nu_m^A\\ \nu_m^B\end{bmatrix} = [P_{cd}]\nu_d \triangleq \begin{bmatrix}P_{md}^A\\ P_{md}^B\end{bmatrix}\nu_d \tag{14}$$

where ν_d denotes a minimum set of generalized coordinates of a statically complete reduced-order system. To obtain the reduced-order system equations of motion, we substitute $\nu_m^A = P_{md}^A\nu_d$ and $\nu_m^B = P_{md}^B$, into Eq. (10), premultiplying the resultant equations by $P_{md}^{A^T}$ and $P_{md}^{B^T}$, respectively, and summing the resultant equations give

$$M_{dd}\ddot{\nu}_d + \tilde{C}_{dd}\dot{\nu}_d + K_{dd}\nu_d = G_{da}u_a$$
$$y_s = H_{sd}\nu_d \tag{15}$$

where $M_{dd} = P_{md}^{A^T}P_{md}^A + P_{md}^{B^T}P_{md}^B$, with similar expressions for $\tilde{C}_{dd}$, K_{dd}, G_{da}, and H_{sd}. Let $(\Phi_{dd},\Lambda_{dd}) = \text{eig}(K_{dd},M_{dd})$. Equation (15) becomes

$$I_{dd}\ddot{\chi}_d + C_{dd}\dot{\chi}_d + \Lambda_{dd}\chi_d = \Phi_{dd}^T G_{da}u_a \tag{16}$$

$$y_s = H_{sd}\Phi_{dd}\chi_d \tag{17}$$

where χ_d is the generalized coordinate, i.e., $\nu_d = \Phi_{dd}\chi_d$, $\Phi_{dd}^T M_{dd}\Phi_{dd} = I_{dd}$, $C_{dd} = \Phi_{dd}^T\tilde{C}_{dd}\Phi_{dd}$, and $\Lambda_{dd} = \Phi_{dd}^T K_{dd}\Phi_{dd}$ is a diagonal matrix with the squared reduced-order system frequencies along its diagonal. It was proven in Ref. 3 that Φ_{ek} [cf., Eq. (7)] are captured exactly in Φ_{dd} in spite of augmenting the composite mode set with static correction modes. The matrix Λ_{dd} also contains a number of extraneous modes.[2,3,12,13]

The system damping matrix C_{dd} in Eq. (16), in general, is not a diagonal matrix. However, it is desirable to have a diagonal C_{dd} with the following properties: 1) a set of system modes has a uniform damping of, say, 0.25%; and 2) the set of unwanted extraneous modes has damping factors larger than a preselected level.

Once C_{dd} is selected, the question then becomes, what should the component damping matrices C_{mm}^A and C_{mm}^B be to approximate the selected C_{dd}?

III. Component Modes Damping Assignment Methodology

A. Relation Between the Component and System Damping Matrices

A relation between the component and system damping matrices must first be established to address the problem we have on hand. To establish that relation, we first note from Eq. (14) that

$$\nu_m^A = P_{md}^A\nu_d = P_{md}^A\Phi_{dd}\chi_d \triangleq Q_{md}^A\chi_d$$

Similarly,

$$\nu_m^B = P_{md}^B\Phi_{dd}\chi_d \triangleq Q_{md}^B\chi_d$$

Substituting these relations into Eq. (10), premultiplying the resultant equations by $Q_{md}^{A^T}$ and $Q_{md}^{B^T}$, respectively, equating the sum of the resultant equations to Eq. (16), and comparing like terms gives

$$Q_{md}^{A^T}Q_{md}^A + Q_{md}^{B^T}Q_{md}^B = I_{dd} \tag{18}$$

$$Q_{md}^{A^T}C_{mm}^A Q_{md}^A + Q_{md}^{B^T}C_{mm}^B Q_{md}^B = C_{dd} \tag{19}$$

$$Q_{md}^{A^T}\Lambda_{mm}^A Q_{md}^A + Q_{md}^{B^T}\Lambda_{mm}^B Q_{md}^B = \Lambda_{dd} \tag{20}$$

These equations may be rewritten as follows. Let us denote Q^A_{md} and Q^B_{md} by

$$Q^{A^T}_{md} = [Q^{A_1}_{d1} \quad Q^{A_2}_{d1} \quad \cdots \quad Q^{A_m}_{d1}] \tag{21}$$

$$Q^{B^T}_{md} = [Q^{B_1}_{d1} \quad Q^{B_2}_{d1} \quad \cdots \quad Q^{B_m}_{d1}] \tag{22}$$

Here, $Q^{A_i}_{d1}$ and $Q^{B_j}_{d1}$, i and $j = 1, \ldots, m$, are $d \times 1$ vectors. Let us further define

$$R^{A_i}_{dd} = Q^{A_i}_{d1} Q^{A_i^T}_{d1} \tag{23}$$

$$R^{B_j}_{dd} = Q^{B_j}_{d1} Q^{B_j^T}_{d1} \tag{24}$$

where $R^{A_i}_{dd}$, $i = 1, \ldots, m$, and $R^{B_j}_{dd}$, $j = 1, \ldots, m$, are $d \times d$ rank one symmetric matrices. The substitutions of Eqs. (21–24) into Eqs. (18–20) give the following matrix algebraic relations[14]:

$$\sum_{i=1}^{i=m} R^{A_i}_{dd} + \sum_{j=1}^{j=m} R^{B_j}_{dd} = I_{dd} \tag{25}$$

$$\sum_{i=1}^{i=m} c_{A_i} R^{A_i}_{dd} + \sum_{j=1}^{j=m} c_{B_j} R^{B_j}_{dd} = C_{dd} \tag{26}$$

$$\sum_{i=1}^{i=m} \omega^2_{A_i} R^{A_i}_{dd} + \sum_{j=1}^{j=m} \omega^2_{B_j} R^{B_j}_{dd} = \Lambda_{dd} \tag{27}$$

To arrive at Eq. (26), we have assumed that the component damping matrices are diagonal, that is, $C^A_{mm} = \text{diag}[c_{A_1}, \ldots, c_{A_m}]$ and $C^B_{mm} = \text{diag}[c_{B_1}, \ldots, c_{B_m}]$. This assumption has been made only for convenience. If, for example, the (1,2) and (2,1) components of C^A_{mm} (denoted by $c_{A_{12}}$) are nonzero, then the term

$$c_{A_{12}}(Q^{A_1}_{d1} Q^{A_2^T}_{d1} + Q^{A_2}_{d1} Q^{A_1^T}_{d1})$$

must be added to the left-hand side of Eq. (26). Given a system damping matrix C_{dd} with certain desirable properties, an optimization problem that determines the values of c_{A_i} and c_{B_j} (i and $j = 1, \ldots, m$) that best satisfies Eq. (26) will be described in Sec. III.B. Clearly, the additions of terms due to nonzero off-diagonal elements of C^A_{mm} and C^B_{mm} in Eq. (26) will increase the degree of freedom of the optimization problem. The larger the degree of freedom of the optimization problem, the better we can equal the left-hand side of Eq. (26) to the desired C_{dd} matrix.

With reference to Eqs. (26) and (27), $R^{A_i}_{dd}$ may be interpreted as a relative contribution matrix that determines the contribution of the damping factor of the ith mode of reduced-order component A model to the system damping matrix, whereas $R^{B_j}_{dd}$ determines that contributed by the jth mode of the reduced-order component B model. Note from Eq. (25) that the sum of these relative contribution matrices is an identity matrix.

B. Solving an Unconstrained Optimization Problem

Given a desired system damping matrix C_{dd} with certain desirable properties, the optimal values of c_{A_i} and c_{B_j} (i or $j = 1, \ldots, m$) that best satisfy Eq. (26) may be determined. To that end, consider the minimization of a cost functional J

$$\min_{c_{A_i}, c_{B_j}} J = \frac{1}{2} \left\| C_{dd} - \sum_{i=1}^{i=m} c_{A_i} R^{A_i}_{dd} - \sum_{j=1}^{j=m} c_{B_j} R^{B_j}_{dd} \right\|^2_F \tag{28}$$

where $\| \cdot \|^2_F$ is the squared Frobenius norm of the matrix concerned. The cost functional J can also be written as

$$J = \frac{1}{2} \sum_{r=1}^{r=d} \sum_{s=1}^{s=d} \alpha^2_{rs} \tag{29}$$

where

$$\alpha_{rs} = [C_{dd}]_{rs} - \sum_{i=1}^{i=m} c_{A_i} [R^{A_i}_{dd}]_{rs} - \sum_{j=1}^{j=m} c_{B_j} [R^{B_j}_{dd}]_{rs} \tag{30}$$

where r and $s = 1, \ldots, d$. The optimality condition of this minimization problem is

$$\frac{\partial J}{\partial c_{A_i}} = \frac{\partial J}{\partial c_{B_j}} = 0 \tag{31}$$

where i and $j = 1, \ldots, m$. Hence, the optimal values of c_{A_i} and c_{B_j} are

$$[c_{A_1}, \quad c_{A_2}, \ldots, c_{B_1}, \quad c_{B_2}, \ldots]^T = E^{-1} \times f \tag{32}$$

where E is a $2m \times 2m$ matrix and f is a $2m \times 1$ matrix

$$E = \begin{bmatrix} \|R^{A_1}_{dd} R^{A_1}_{dd}\| & .. & \|R^{A_1}_{dd} R^{A_m}_{dd}\| & .. & \|R^{A_1}_{dd} R^{B_m}_{dd}\| \\ \|R^{A_2}_{dd} R^{A_1}_{dd}\| & .. & \|R^{A_2}_{dd} R^{A_m}_{dd}\| & .. & \|R^{A_2}_{dd} R^{B_m}_{dd}\| \\ .. & .. & .. & .. & .. \\ \|R^{B_m}_{dd} R^{A_1}_{dd}\| & .. & \|R^{B_m}_{dd} R^{A_m}_{dd}\| & .. & \|R^{B_m}_{dd} R^{B_m}_{dd}\| \end{bmatrix} \tag{33}$$

$$f = \begin{bmatrix} \|R^{A_1}_{dd} C_{dd}\| \\ \cdots \\ \|R^{A_m}_{dd} C_{dd}\| \\ \|R^{B_1}_{dd} C_{dd}\| \\ \cdots \\ \|R^{B_m}_{dd} C_{dd}\| \end{bmatrix} \tag{34}$$

Here

$$\|XY\| = \sum_{i=1}^{n} \sum_{j=1}^{n} X_{ij} \times Y_{ij}$$

in Eqs. (33) and (34). Using a generalized form of Cauchy's inequality theorem,[15] it can be shown that the determinant of E is always greater than zero (i.e., $|E| > 0$) unless the matrices $R^{A_1}_{dd}, \ldots, R^{A_m}_{dd}, \ldots, R^{B_m}_{dd}$ are linearly dependent. That is, unless there are numbers $x, y, \ldots, w$, not all zero, such that

$$x R^{A_1}_{dd} + y R^{A_2}_{dd} + \cdots + w R^{B_m}_{dd} = O_{dd}$$

In that case, a SVD procedure can be used to select a reduced set of independent modes from the original set before applying this technique. When the matrices $R^{A_1}_{dd}, \ldots, R^{B_m}_{dd}$ are independent, $|E| > 0$, and the unknowns c_{A_i} and c_{B_j} can always be determined by Eq. (32).

The preceding optimization problem could be modified if we want to stress the importance of having smaller diagonal terms in $[\alpha_{rs}]$[see Eq. (30)]. To this end, let us introduce a symmetric weighting matrix W in Eq. (29)

$$J_W = \frac{1}{2} \sum_{r=1}^{r=d} \sum_{s=1}^{s=d} W^2_{rs} \alpha^2_{rs} \tag{35}$$

When the diagonal elements of the matrix W are assigned (relatively) larger weightings than those given to the off-diagonal terms, diagonal elements of the optimized $[\alpha_{rs}]$ will be smaller than the off-diagonal terms. This ensures that the desired damping factors (of, e.g., 0.25%) of the selected system modes are achieved. However, this is at the expense of having larger off-diagonal terms in the resultant system damping matrix. One way to select a compromise weighting matrix that balances the diagonal and off-diagonal terms will be described via an example (see Sec. IV).

The minimization of the modified cost function J_W may be solved using modified versions of the technique just described.

C. Solving a Constrained Optimization Problem

Results obtained from the unconstrained optimization problem [see Eq. (28)] might or might not be physically mean-

Table 1 Frequencies of full-order system flexible modes at a clock angle of 300 deg

Mode	Ω_{system}, Hz	Mode	Ω_{system}, Hz	Mode	Ω_{system}, Hz
1	0.127	31	5.634	61	9.606[a]
2	0.864[a]	32	5.652	62	10.179
3	1.227	33	5.652	63	10.306
4	1.236[a]	34	5.660	64	10.420[a]
5	1.238	35	5.660	65	10.555[a]
6	1.479[a]	36	5.662	66	13.534[a]
7	1.522	37	5.783	67	13.990
8	1.546	38	5.785	68	16.800[a]
9	1.602	39	5.809	69	16.996
10	1.707[a]	40	5.814	70	17.122
11	1.734[a]	41	5.824	71	17.977
12	2.072[a]	42	5.824	72	18.063
13	2.341	43	5.830	73	18.083
14	2.351[a]	44	5.830	74	18.186
15	2.815[a]	45	5.833	75	18.527
16	3.073	46	5.833	76	18.688
17	3.232	47	5.834	77	19.591
18	3.233	48	5.834	78	19.593
19	3.707[a]	49	5.835	79	21.280[a]
20	4.172	50	5.835	80	27.537
21	4.977	51	5.835	81	29.919
22	5.022	52	5.839	82	31.083
23	5.231[a]	53	5.901	83	55.686
24	5.247	54	6.034	84	67.384
25	5.455	55	6.161	85	71.770[a]
26	5.455	56	6.221	86	82.129[a]
27	5.467[a]	57	6.869	87	87.522
28	5.588	58	7.056[a]	88	96.235
29	5.588	59	7.190	89	100.95
30	5.633	60	8.153[a]	90	274.45

[a]Flexible system modes in the composite mode set.

Table 2 Frequencies of reduced-order stator, rotor, and system flexible modes at a clock angle of 300 deg

Flexible mode	ω_{stator}, Hz	ω_{rotor}, Hz	ω_{system}, Hz
1	7.105	0.143	0.127
2	9.129	0.866	0.864[a]
3	10.561	1.237	1.236[a]
4	14.560	1.483	1.479[a]
5	43.172	1.728	1.707[a]
6	50.070	2.286	1.734[a]
7	63.530	2.809	2.072[a]
8	80.867	3.647	2.351[a]
9	86.989	3.996	2.815[a]
10	96.605	5.207	3.707[a]
11	166.340	5.337	4.167
12	240.180	5.994	5.231[a]
13	254.520	6.410	5.433
14		9.503	5.467[a]
15		10.291	6.150
16		10.553	6.436
17		13.536	7.056[a]
18		15.613	8.153[a]
19		29.188	9.606[a]
20		41.181	9.613
21		58.524	10.294
22		69.003	10.420[a]
23		77.722	10.555[a]
24			13.534[a]
25			13.997
26			15.860
27			16.800[a]
28			20.591
29			21.280[a]
30			28.462
31			34.316
32			41.214
33			48.011
34			58.318
35			71.770[a]
36			82.129[a]

[a]Exactly captured system flexible modes (cf., Table 1).

ingful. Situations arise in which, for a given C_{dd}, one or more of c_{A_i} and c_{B_j} (i or $j = 1,\ldots, m$) might not be positive. (If $C_{dd} = \beta_1 I_d + \beta_2 \Lambda_{dd}$, where both β_1 and β_2 are positive constants, then the solutions of all of the c_{A_i} and c_{B_j} are guaranteed to be positive.) While positive c_{A_i} and c_{B_i} values imply energy dissipation, a negative c_{A_i}, for example, implies the addition of energy to the structure, a situation that is only possible with active control.

To overcome this difficulty, the formulated optimization problem may be modified with the additions of $4m$ inequality constraints

$$\begin{aligned} 1 \geq c_{A_i}/[2\omega_{A_i}] \geq 0, \qquad i = 1,\ldots, m \\ 1 \geq c_{B_j}/[2\omega_{B_j}] \geq 0, \qquad j = 1,\ldots, m \end{aligned} \tag{36}$$

The additions of these inequality constraints make it impossible to solve the optimization problem analytically [see Eq. (32)]. However, the constrained problem can be solved iteratively using, for example, the Fortran package for nonlinear programming, NPSOL.[16] This is a package that is designed to minimize a smooth function subject to constraints, which may include simple bounds on the variables [see Eq. (36)], linear constraints, and smooth nonlinear constraints. The effectiveness of NPSOL has been validated in numerous prior studies.

IV. Applying ModeDamp on a High-Order, Finite Element Galileo Model

The effectiveness of the modes damping assignment methodology (ModeDamp) will now be demonstrated using a high-order finite element model of the cruise-configured Galileo spacecraft. The three-body topology of the dual-spin Galileo spacecraft is illustrated in Fig. 2.[2] The rotor is the largest and most flexible component represented with 243 DOF. The smaller and more rigid stator is represented with 57 DOF; the scan platform is the smallest body idealized as rigid with 6 DOF.

For the purpose of controller design, low-order system models, at all configurations of interest, over a frequency range of interest (0–10 Hz) are needed. To this end, we apply the MacNeal-Rubin (M-R) version of the COMPARE methodology on the Galileo model. (The Craig-Brampton version is equally applicable.) The first stage of COMPARE requires the generations of MacNeal-Rubin mode sets for all of the flexible components. Following standard procedures, free interface normal modes of both the rotor and stator are first determined and then truncated at twice the frequency of interest (20 Hz). Next, these truncated normal mode sets are each augmented with residual modes. These M-R mode sets are then used to generate the needed CMS-based reduced-order models of both the rotor and the stator.

Next, the CMS-based component models together with the interface compatibility conditions are used to construct system

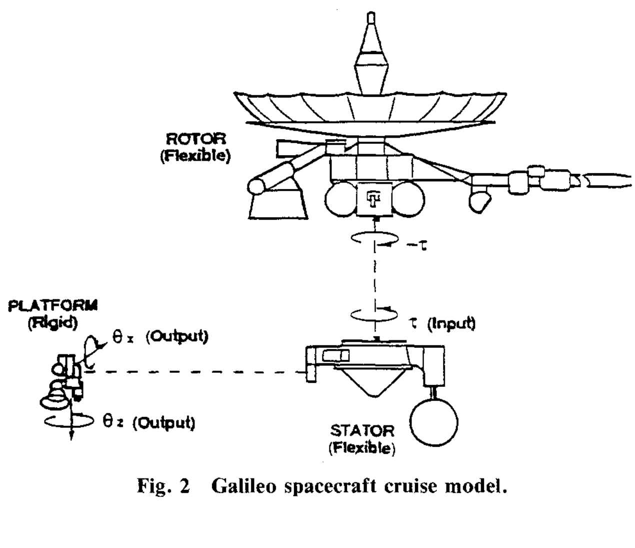

Fig. 2 Galileo spacecraft cruise model.

models at all system configurations of interest. Using the modal influence coefficient[2] as a selection criterion, important system modes are picked at system configurations with clock angles of 0, 60, 120, 180, 240, and 300 deg. A composite mode set that encompasses important modes at all configurations is then determined. This set, with 8 rigid-body and 21 flexible modes, is indicated in Table 1.

The next step is to augment the composite mode set with static correction mode(s). For the Galileo example, we augment the composite mode set with two residual modes, one for an imput torque about the Z axis on the rotor side of the rotor/stator interface and a second for an equal and opposite torque on the stator side of the interface. The enlarged mode set is then projected onto the flexible components, and a SVD was used to remove linearly dependent modes in the projected stator mode set. The resultant reduced-order models of the rotor and stator have 29 (with 6 rigid body) and 21 (with 8 rigid body) modes, respectively. The assembled reduced-order model has 44 (with 8 rigid body) modes. The natural frequencies of these reduced-order component models and those for a system model at a clock angle of 300 deg are tabulated in Table 2. Note that all of the system flexible modes retained in the composite mode set have been captured exactly in the

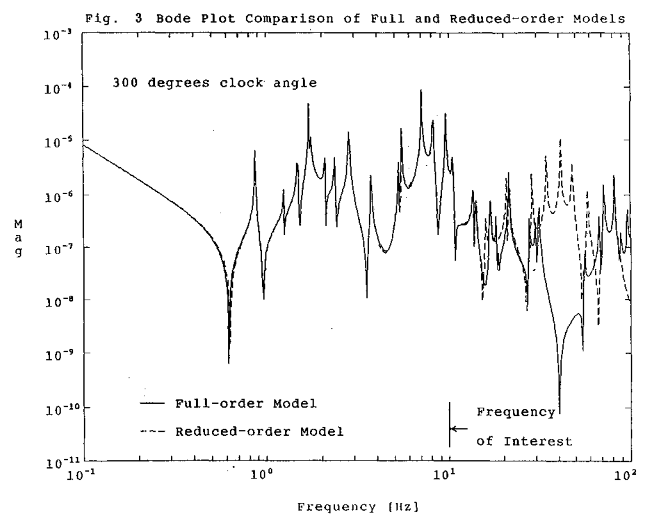

Fig. 3 Bode plot comparison of the full- and reduced-order models.

Table 3 Damping factors of the rotor and stator flexible modes

Mode	Rotor freq., Hz	Rotor ζ, %	Stator freq., Hz	Stator ζ, %
1	0.143	0.4799	7.105	0.3791
2	0.866	0.2505	9.129	0.1638
3	1.237	0.2508	10.561	0.2474
4	1.483	0.2502	14.560	0.6307
5	1.728	0.4116	43.172	1.0851
6	2.286	0.3238	50.070	0.9665
7	2.809	0.2514	63.530	2.1919
8	3.647	0.2214	80.867	3.1790
9	3.996	0.7162	86.989	0.4047
10	5.207	0.2435	96.605	2.1883
11	5.337	0.3111	166.340	10.0110
12	5.994	0.4924	240.180	6.8794
13	6.410	0.7881	254.520	5.4772
14	9.503	0.6807		
15	10.291	0.0070		
16	10.553	0.2503		
17	13.536	0.3060		
18	15.613	0.9075		
19	29.188	0.9720		
20	41.181	1.2991		
21	58.524	1.3902		
22	69.003	2.0869		
23	77.722	2.8904		

reduced-order system model. A Bode plot comparison of the full- and reduced-order models, at a clock angle of 300 deg, shows excellent result (cf., Fig. 3). Matches made at all other clock angles are equally impressive.[6]

The ModeDamp methodology is now employed to determine appropriate damping levels for all the rotor and stator's flexible modes so as to produce a desirable system damping matrix C_{dd}. But what constitutes a desirable C_{dd}? We might, for example, want a C_{dd} with modal damping factors closely matching those found experimentally. To this end, we could use the experimentally determined modal damping factors of the TOPEX/Poseidon satellite[17]: 1.0% for $5 \leq \omega \leq 8.5$ Hz, 0.5% for $8.5 \leq \omega \leq 11$ Hz, 1.0% for $11 \leq \omega \leq 35$ Hz, etc. In our research, the target C_{dd} is assumed diagonal, with the following properties:

1) There must be a uniform damping of 0.25% for all of the recaptured system modes that fall within the frequency range of interest (0–10 Hz); that is, $\zeta_i = 0.25\%$, for i = 2–10, 12, 14, 17, 18, and 19 (cf., Tables 2 and 4).

2) The damping factors of all of the recaptured system modes that fall outside the frequency range of interest must be at least 0.25%; that is, $\zeta_j \geq 0.25\%$ for j = 1, 22–24, 27, 29, 35, and 36.

3) No specific requirement is made on the damping factors of all of the remaining system modes.

These requirements on the damping factors of the system modes are explained as follows. The recaptured system modes are modes that make significant contributions to the system input-to-output mapping. It is desirable to have a uniform 0.25% damping factor for all of the important recaptured system modes below 10 Hz, which closely approximates the

Table 4 Damping factors of the reassembled system's flexible modes

Mode	ω_{sys}, Hz	Mode set 1 ζ_{sys}, %	Mode set 2 ζ_{sys}, %	Mode set 3 ζ_{sys}, %
1	0.127		0.4261	
2	0.864[a]	0.2500		
3	1.236[a]	0.2500		
4	1.479[a]	0.2487		
5	1.707[a]	0.1850		
6	1.734[a]	0.2795		
7	2.072[a]	0.1607		
8	2.351[a]	0.2748		
9	2.815[a]	0.2503		
10	3.707[a]	0.2520		
11	4.167			0.6438
12	5.231[a]	0.2503		
13	5.433			0.3103
14	5.467[a]	0.2401		
15	6.150			0.4784
16	6.436			0.7833
17	7.056[a]	0.2332		
18	8.153[a]	0.2577		
19	9.606[a]	0.2602		
20	9.613			0.6782
21	10.294			0.0090
22	10.420[a]		0.2500	
23	10.555[a]		0.2505	
24	13.534[a]		0.3070	
25	13.997			0.5977
26	15.860			0.8979
27	16.800[a]		0.6157	
28	20.591			0.3918
29	21.280[a]		0.8268	
30	28.462			0.7813
31	34.316			1.0344
32	41.214			1.2990
33	48.011			1.2128
34	58.318			1.6181
35	71.770[a]		2.2640	
36	82.129[a]		2.1006	

[a]Exactly captured flexible system modes in the reduced-order system model. Damping factors in these mode sets must be close to 0.25% in mode set 1, higher than 0.25% in mode set 2, and between 0 and 100% in mode set 3.

level commonly and conservatively assumed for large space structures. Recaptured system modes that fall outside the frequency range of interest are of less importance. However, a damping factor of at least 0.25% is preferred because they can damp out the transient dynamics due to these modes. All of the remaining system modes make little contribution to the system input-to-output mapping and may have any nonzero damping factors.

Having selected the described damping matrix C_{dd}, it should be emphasized here that any other appropriately selected C_{dd}, diagonal or nondiagonal, can also be used. For example, in Ref. 18, all of the recaptured system modes of a 28-DOF structure were assigned a uniform damping factor of 0.25% whereas the highest frequency extraneous mode was assigned a larger damping factor of 10%.

To realize requirements 1–3, the 36×36 symmetric weighting matrix W must be carefully selected. First, the diagonal elements of W are selected with $W(i,i) = \zeta_2\omega_2/\zeta_i\omega_i$ ($i = 2$–10, 10, 12, 14, 17, 18, and 19), and $W(i,i) = 0$ for all of the remaining system modes. These selections will give equal weighting to all of the recaptured system modes below 10 Hz, paying no attention to the remaining modes. The off-diagonal elements of the ith row of W are assigned the value $W_{\text{off}} = pW(i,i)$, where $p = 0.11$. If W_{off} is small, i.e., we are paying less attention to these off-diagonal terms, and we can achieve the desired 0.25% damping level almost exactly. However, the magnitudes of some of the off-diagonal terms of C_{dd} might be larger than the corresponding diagonal terms. The matrix C_{dd} is no longer diagonally dominant, against what we want. Conversely, if W_{off} has a larger value, we will approach a truly diagonally dominant C_{dd}, but the required damping levels for the diagonal terms in C_{dd} cannot be met closely. The selected value of p is a trial-and-error compromise.

Inequality constraints on the component damping factors, such as those mentioned in Sec. III.C should always be enforced. That is,

$$1 \geq c_i^R/[2\omega_i^R] \geq 0, \qquad i = 1,\ldots, 23$$
$$1 \geq c_j^S/[2\omega_j^S] \geq 0, \qquad j = 1,\ldots, 13 \qquad (37)$$

In addition, we must establish new system-level inequality constraints to implement requirements 2 and 3. These constraints take the form of [see Eq. (26)]

$$\text{diag}(C^U) \geq \text{diag}\left(\sum_{i=1}^{i=23} c_i^R R_i^R + \sum_{j=1}^{j=13} c_j^S R_j^S\right) \geq \text{diag}(C^L) \qquad (38)$$

where C^U and C^L are upper and lower matrix bounds on the system damping matrix. The matrix C^U is a diagonal matrix $\text{diag}(2 \times 1 \times [\omega_1^{\text{sys}},\ldots, \omega_{36}^{\text{sys}}]^T)$. That is, the damping factors of all of the system modes should be less than unity. Similarly, C^L is a diagonal matrix $\text{diag}(2 \times 0 \times [\omega_1^{\text{sys}},\ldots, \omega_{36}^{\text{sys}}]^T)$, except for modes $j = 1$, 22–24, 27, 29, 35, and 36, which should have lower bounds of $2 \times 0.0025 \times \omega_j^{\text{sys}}$.

The damping factors of both the rotor and the stator are now determined using the ModeDamp methodology. The results are tabulated in Table 3. The resultant damping factors of the reduced-order system modes are given in Table 4. As indicated in Table 4, the damping factors of all of the recaptured system modes below 10 Hz are indeed close to the desired 0.25% level. The damping factors of modes 5 and 7, at 0.1850 and 0.1607%, respectively, could be made closer to the desired 0.25% level by increasing the weighting factors on these modes. However, the damping factors of other modes in that mode set 1 might deviate from 0.25%. The damping factors of all of the recaptured system modes above 10 Hz (ranging from 0.2500 and 2.2640%) are all above the desired 0.25% level. The resultant C_{dd} matrix is also diagonally dominant. In fact, if $r_i = \max_{j=1,\ldots,36, j\neq i}|c_{ij}/c_{ii}|$ represents the maximum of all ratios of the off-diagonal terms to the diagonal term, for mode $i = 2$–10, 12, 14, and 17–19 (important system modes), then r_i are given by 0.49, 0.17, 0.07, 0.12, 0.47, 0.07, 0.04, 0.36, 0.40, 0.02, 0.27, 0.11, 0.06, and 0.35, respectively.

V. Concluding Remarks

To simulate the dynamical motion of articulated, multiflexible body structures, one can use multibody simulation packages such as DISCOS. To this end, one must supply appropriate reduced-order models for all of the flexible components involved. The component modes projection and assembly model reduction methodology is one way to construct these reduced-order component models. In conjunction, we must also supply component damping matrices that when reassembled generate a system damping matrix that has certain desirable properties. The problem of determining the damping factors of components' modes given a system damping matrix is addressed here.

To begin with, we must establish from first principles a matrix-algebraic relation between the system's modal damping matrix and the components' modal damping matrices. An unconstrained/constrained optimization problem can then be formulated to determine the component modes' damping factors that best satisfy that matrix-algebraic relation. In this research, the proposed technique, called ModeDamp, has been specialized to cases where the component modes are obtained by the component modes projection and assembly model reduction methodology. However, this technique can be easily adapted to cases where the component modes are determined using an alternative methodology. A high-order finite element model of the Galileo spacecraft was used to successfully validate the effectiveness of the developed damping assignment methodology. When properly implemented, this methodology aids dynamicists in their studies of damped dynamics of interconnected flexible bodies using multibody simulation packages.

Acknowledgments

The research described here was conducted at Jet Propulsion Laboratory, California Institute of Technology under contract with NASA. The author wishes to thank his colleagues D. Bernard, F. Hadaegh, R. Laskin, G. Macala, G. Man, S. Sirlin, J. Spanos, W. Tsuha, and M. Wette; J. Storch at the Charles Stark Draper Laboratory; and A. von Flotow, formerly with the Massachusetts Institute of Technology, for many helpful discussions and valuable suggestions. All errors are my responsibility.

References

[1]Bodley, C. S., Devers, A. D., Park, A. C., and Frisch, H. P., "A Digital Computer Program for the Dynamic Interaction Simulation of Controls and Structure (DISCOS)," NASA TP 1219, Vols. I and II, May 1978.

[2]Lee, A. Y., and Tsuha, W. S., "An Enhanced Projection and Assembly Model Reduction Methodology," *Proceedings of the AIAA Guidance, Navigation, and Control Conference* (New Orleans, LA), AIAA, Aug. 1991, Washington, DC, 1991, pp. 1350–1359 (AIAA Paper 91-2749).

[3]Lee, A. Y., and Tsuha, W. S., "A Component Modes Projection and Assembly Model Reduction Methodology for Articulated, Multiflexible Body Structures," *Proceedings of the AIAA Guidance, Navigation, and Control Conference* (Hilton Head, SC), AIAA, Washington, DC, 1992, pp. 143–153 (AIAA Paper 92-4323).

[4]Lee, A. Y., "The COMPACT Model Reduction Methodology for Articulated, Multiflexible Body Structures," Jet Propulson Lab., JPL Internal Document EM-1271, Pasadena, CA, Aug. 1992.

[5]Hasselman, T. K., "Damping Synthesis from Substructure Tests," *AIAA Journal,* Vol. 14, No. 10, 1976, pp. 1409–1418.

[6]Béliveau, J. G., and Soucy, Y., "Damping Synthesis Using Complex Substructure Modes and a Hermitian System Representation," *AIAA Journal,* Vol. 23, No. 12, 1985, pp. 1952–1956.

[7]Béliveau, J. G., and Rong, H., "Damping Synthesis Using Residual Free Interface Inertia Relief Complex Attachment Modes," *Proceedings of the AIAA/ASME/ASCE/AHS/ASC 32nd Structures,*

Structural Dynamics, and Materials Conference (Baltimore, MD), AIAA, Washington, DC, 1991, pp. 2472–2478 (AIAA Paper 91-0993).

[8]Huston, D. R., Graves, W. R., and Béliveau, J. G., "Experimental Verification of Complex Component Mode Synthesis," *Proceedings of the AIAA/ASME/ASCE/AHS/ASC 32nd Structures, Structural Dynamics, and Materials Conference* (Baltimore, MD), AIAA, Washington, DC, 1991, pp. 2441–2451 (AIAA Paper 91-0944).

[9]Lim, K. B., Maghami, P. G., and Joshi, S. M., "Comparison of Controller Design for an Experimental Flexible Structure," *IEEE Control Systems*, Vol. 12, No. 3, 1992, pp. 108–118.

[10]Macala, G., "A Modal Reduction Method for Use With Nonlinear Simulations of Flexible Multibody Spacecraft," *Proceedings of the AIAA/AAS Astrodynamics Conference* (Seattle, WA), AIAA, New York, 1984 (AIAA Paper 84-1989).

[11]Craig, R. R., Jr., *Structural Dynamics: An Introduction to Computer Methods*, Wiley, New York, 1981.

[12]Lee, A. Y., and Tsuha, W. S., "Applying the Enhanced Projection and Assembly Model Reduction Methodology on Articulated, Multi-flexible Body Structures," *Proceedings of the IEEE Singapore International Conference on Intelligent Control and Instrumentation*, IEEE Singapore Section, Singapore, Feb. 1992, pp. 597–602.

[13]Bernard, D., "Projection and Assembly Method for Multibody Component Model Reduction," *Journal of Guidance, Control, and Dynamics*, Vol. 13, No. 5, 1990, pp. 905–912.

[14]Lee, A. Y., "The Component Modes Damping Assignment Techniques," Jet Propulsion Lab., JPL Internal Document D-7330, Pasadena, CA, April 1990.

[15]Hardy, G. H., Littlewood, J. E., and Pólya, G., *Inequalities*, Cambridge Univ. Press, 2nd ed., Cambridge, England, UK, 1959, p. 16.

[16]Gill, P. E., Murray, W., Saunders, M., and Wright, M. H., "User's Guide for NPSOL (4.0): A Fortran Package for Nonlinear Programming," System Optimization Lab., Dept. of Operations Research, TR SOL 86-2, Stanford Univ., Stanford, CA, 1986.

[17]Larkin, P. A., Francis, J. T., Robinson, F. Y., and Lou, M., "Structural Development of the TOPEX/POSEIDON Satellite," *Sound and Vibration*, Vol. 26, No. 8, 1992, pp. 14–23.

[18]Lee, A. Y., "A Component Modes Damping Assignment Methodology (ModeDamp) for Articulated, Multi-flexible Body Structures," Jet Propulsion Lab., JPL Internal Document EM 343-1289, Pasadena, CA, Sept. 1992.